PHYSICAL REVIEW B **86**, 134430 (2012)

Quantum torus chain

M. P. Qin,[1] J. M. Leinaas,[2] S. Ryu,[3] E. Ardonne,[4,5] T. Xiang,[1,6] and D.-H. Lee[7,8]

[1]*Institute of Physics, Chinese Academy of Sciences, P.O. Box 603, Beijing 100190, China*

[2]*Department of Physics, University of Oslo, P.O. Box 1048 Blindern, N-0316 Oslo, Norway*

[3]*Department of Physics, University of Illinois at Urbana-Champaign, 1110 West Green Street, Urbana, Illinois 61801-3080, USA*

[4]*Nordita, Royal Institute of Technology and Stockholm University, Roslagstullsbacken 23, SE-10691 Stockholm, Sweden*

[5]*Department of Physics, Stockholm University, AlbaNova University Center, SE-10691 Stockholm, Sweden*

[6]*Institute of Theoretical Physics, Chinese Academy of Sciences, P.O. Box 2735, Beijing 100190, China*

[7]*Department of Physics, University of California at Berkeley, Berkeley, California 94720, USA*

[8]*Materials Sciences Division, Lawrence Berkeley National Laboratory, Berkeley, California 94720, USA*

(Received 21 May 2012; revised manuscript received 4 October 2012; published 26 October 2012)

We introduce a set of one-dimensional quantum lattice models which we refer to as the *quantum torus chain*. These models have discrete global symmetry and *projective* on-site representations. They possess an integer-valued parameter which controls the presence or absence of frustration. Depending on whether this parameter is even or odd, these models exhibit either gapped symmetry-breaking phases with isolated critical points or gapped symmetry-breaking phases separated by gapless *phases*. We discuss the property of these phases and phase transitions for two special values of the parameter and point out many open problems.

DOI: 10.1103/PhysRevB.86.134430 PACS number(s): 75.10.Pq, 75.10.Jm, 64.70.Tg

I. INTRODUCTION

Over the years, many interesting lattice models have been introduced to capture the essence of important physical concepts and make them open for more quantitative studies. In modern language, quantum lattice models can capture short-range entangled states such as symmetry-breaking or symmetry-protected topological states.[1] They also can capture long-range entangled states such as the quantum critical and "intrinsic topological ordered" states.

The importance of symmetry is well known in classical and quantum physics. Recently, it was realized that a strong tie exists between quantum entanglement and symmetry.[1] For example, in one space dimension, Chen *et al.*[1] showed that short-range, entangled, fully symmetric quantum states are classified by the *projective* representation of the internal symmetry group. In addition, if the site representation of the symmetry group is *projective*, then short-range entanglement is impossible without symmetry breaking. Because in one dimension a gapped system is necessarily short-range entangled, this implies that *projective* on-site representation cannot have an energy gap without breaking some symmetry. This result is a generalization of Haldane's work on the SO(3) spin chain.[2] There, half-integer spin chains need to break a symmetry to open an energy gap, while integer spin chains do not.

In this paper, we introduce a family of one-dimensional quantum lattice models whose global symmetry groups are discrete and the on-site representation is projective. Indeed, these models are either gapless or exhibit spontaneous symmetry breaking. In addition, they possess an integer-valued parameter which controls the presence or absence of frustration. Depending on whether this parameter is even or odd, qualitatively different phase diagrams are observed. By applying the density matrix renormalization group (DMRG)[3,4] and Matrix product state (MPS)[5] methods, we find for the even parameter that these models are generically gapped and show spontaneous symmetry breaking. Fine tuning is required to close the energy gap. On the other hand, for the odd parameter, both the gapped symmetry-breaking phase and the gapless symmetric phase are generic. The results are all consistent with the conclusions drawn by Chen *et al.*[1]

The results reported in this paper show that the class of models that we introduced in this paper has a rich set of interesting phases. We hope that the study of this class of models will enhance our understanding of symmetry-protected topological phases in one-dimensional systems and of topological phases in a more general setting.

II. THE QUANTUM TORUS CHAIN

The family of models, which we refer to as the quantum torus chain, is motivated from the following view of the quantum spin chain.

The dimension D of the single-site Hilbert space of a SU(2) spin-S chain is $2S+1$. The basis states can be viewed as the one-particle states of a unit-charged particle running on a sphere enclosing a magnetic monopole which produces $2S$ magnetic-flux quanta through the sphere.[6] The nonzero total Gaussian curvature of the sphere leads to a term in the Hamiltonian which has the same form as the term describing the flux. Thus, the curvature effectively increases the flux, and there are $D=2S+1$ rather than $2S$ one-particle states (see also Ref. 7). The spin operators $S^{x,y,z}$ are the generators of the magnetic translation.

In the *XYZ* model, the nearest-neighboring spin operators are coupled as

$$H_{XYZ}=\sum_i \left(J_x S_i^x S_{i+1}^x + J_y S_i^y S_{i+1}^y + J_z S_i^z S_{i+1}^z\right). \quad (1)$$

This is depicted in Fig. 1(a).

In this work, we consider the "torus chain" [Fig. 1(b)], where the spheres of Fig. 1(a) are replaced by the torus. Because the total Gaussian curvature of a torus is zero, the lowest Landau-level degeneracy is equal to the number of flux quanta through each torus.[7] Unlike the sphere, the magnetic

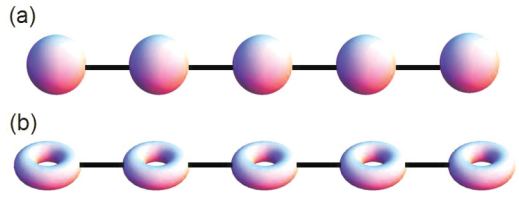

FIG. 1. (Color online) (a) Each site of a quantum spin-S chain can be viewed as the lowest Landau level of a unit-charged particle moving on a sphere under the magnetic field of a Dirac monopole. The total magnetic flux produced by the monopole is $2S$. (b) The Torus chain is a modification of the spin chain where each sphere is replaced by a torus.

translation group of a torus, i.e., the Heisenberg-Weyl group, is *discrete* rather than continuous.[8] The commutation relation between the operators U^x,U^y, which generate the magnetic translations in two orthogonal directions, is

$$U^x U^y = e^{i2\pi/m} U^y U^x, \tag{2}$$

where $(U^x)^m = (U^y)^m = I$. Here, m is the number of flux quanta through each torus and is the integer-valued parameter we referred to earlier. In the following, we shall encounter two different bases, $|q\rangle$ and $|\tilde{q}\rangle$, for the site-Hilbert space. Both q and $\tilde{q}$ are defined modulo m. In the $|q\rangle$ basis, U^x and U^y are given by

$$\begin{aligned} U^x &= \sum_{q=0}^{m-1} e^{i2\pi q/m} |q\rangle\langle q|, \\ U^y &= \sum_{q=0}^{m-1} |q+1\rangle\langle q|. \end{aligned} \tag{3}$$

The dual basis $|\tilde{q}\rangle$ is the Fourier transform of $|q\rangle$, i.e.,

$$|\tilde{q}\rangle = \frac{1}{\sqrt{m}} \sum_{q=0}^{m-1} e^{2\pi i q\tilde{q}/m} |q\rangle.$$

In this basis,

$$\begin{aligned} U^x &= \sum_{\tilde{q}=0}^{m-1} |\tilde{q}+1\rangle\langle\tilde{q}|, \\ U^y &= \sum_{\tilde{q}=0}^{m-1} e^{-2\pi i\tilde{q}/m} |\tilde{q}\rangle\langle\tilde{q}|. \end{aligned} \tag{4}$$

Analogously to the XYZ model, we couple the generators of the magnetic translation group of the torus to form the following Hamiltonian:

$$H = \sum_i \left(\cos\theta U_i^x U_{i+1}^{x\dagger} + \sin\theta U_i^y U_{i+1}^{y\dagger} + \text{H.c.} \right). \tag{5}$$

Here, the parameter θ is introduced to control the relative strength (and sign) between two terms, $\sum_i U_i^x U_{i+1}^{x\dagger} + \text{H.c.}$ and $\sum_i U_i^y U_{i+1}^{y\dagger} + \text{H.c.}$, in the Hamiltonian. In the following, we assume the number of sites L to be an integer multiple of m. With this restriction, the two unitary operators $\mathcal{U}^x = \prod_{i=1}^L U_i^x$ and $\mathcal{U}^y = \prod_{i=1}^L U_i^y$ commute with each other and with the Hamiltonian (5). The Hamiltonian (5) is one of the simplest models which preserves the full group of magnetic translations (the group generated by $\mathcal{U}^x$ and $\mathcal{U}^y$), i.e., an analog of an SU(2) symmetric spin chain. It is possible to consider a further generalization of the model, with the same symmetry, by adding different complex phase factors for the two terms. However, for simplicity, we shall restrict ourselves to the case where the coupling ratio is real. We also note the similarity of our model to the m-state Potts model (although the symmetries are a bit different). For more descriptions of related/similar models, see, e.g., Refs. 9–12.

We will denote the conserved quantum numbers associated with $\mathcal{U}^x$ and $\mathcal{U}^y$ by $(e^{2\pi i Q/m}, e^{-2\pi i\tilde{Q}/m})$ or, more compactly, as $(Q,\tilde{Q})$. In terms of q_i and $\tilde{q}_i$, we have

$$Q = \sum_i q_i \bmod m, \quad \tilde{Q} = \sum_i \tilde{q}_i \bmod m.$$

In addition to $\mathcal{U}^x$ and $\mathcal{U}^y$, there are other symmetry operators that leave the Hamiltonian (5) invariant. First of all, there is the q inversion, $\mathcal{R} = \prod_{i=1}^L R_i$, where

$$R_i|q_i\rangle = |-q_i\rangle \bmod m, \quad R_i|\tilde{q}_i\rangle = |-\tilde{q}_i\rangle \bmod m.$$

Second, there are the anti-unitary operations, K and $\tilde{K} = RK$, which cause complex conjugation in the q and $\tilde{q}$ basis, respectively. We note that $K^2 = \tilde{K}^2 = I$. The operators $\mathcal{U}^x$, $\mathcal{U}^y$, $\mathcal{R}$, and K generate the internal symmetry group G. As one can readily check, the group multiplications of G are identical to those of the symmetry group of a rectangular, periodic lattice on a torus, with $\mathcal{U}^x$ and $\mathcal{U}^y$ as the lattice translations, R as the rotation of angle π, and K and $\tilde{K}$ as the two reflections. We note that as usual, the translation generators of the space group commute. This is because we have restricted L to an integer multiple of m. It is also interesting to note that unlike the usual cases, some of the space-group elements are represented anti-unitarily here. The internal symmetry group G extended with the translations and inversion of the one-dimensional (1D) chain defines the full symmetry group of the Hamiltonian. In addition, the Hamiltonian (5) has a "duality" symmetry upon $\theta \leftrightarrow \pi/2 - \theta \pmod{2\pi}$ and $U^x \leftrightarrow U^y$.

The irreducible representations of the group of internal symmetries determine the (minimal) degeneracies of the energy levels. For example, for $m = 3$, which we shall discuss at great length, the multiplets take the following form in terms of the $(Q,\tilde{Q})$:

$$\begin{aligned} &(Q,\tilde{Q}) = (0,0), \\ &(Q,\tilde{Q}) = (1,0);(2,0), \\ &(Q,\tilde{Q}) = (0,1);(0,2), \\ &(Q,\tilde{Q}) = (1,1);(1,2);(2,1);(2,2). \end{aligned}$$

At the "self-dual" point $\tan\theta = 1$, the two terms in the Hamiltonian (5) have the same coefficient. There, the symmetry group is larger, which causes the two doublets in the above set of equations to become degenerate and form a quadruplet.

III. SOME PROPERTIES FOR GENERAL m

Having introduced the model and its symmetries, we start our analysis by first considering the dependence of the model on the parameter m. It turns out that even and odd m have qualitatively different phase diagrams.

For later discussions, it is useful to consider the subgroup $\mathcal{G}$ generated by the subset of generators that are unitary: $\{I,\mathcal{U}^x,\mathcal{U}^y,\mathcal{R}\}$. This group is isomorphic to the symmetry group of an $m \times m$ oblique lattice on a torus. It is important to note, however, for each site of the 1D chain, this symmetry group is represented by a *projective* representation. The nontrivial U(1) phases are due to the presence of the factor $e^{i2\pi/m}$ in $U^x U^y = e^{i2\pi/m} U^y U^x$. Applying the results of Chen *et al.*, we therefore conclude that Eq. (5) should either exhibit a gapped spectrum with a symmetry-breaking ground state or a gapless spectrum with a symmetric ground state.

To see how this is realized, we first consider the simplest case, with $m = 2$. In this case, we can rewrite Eq. (5) in terms of a spin-1/2 Hamiltonian. This is achieved by identifying $q = 0,1$, with spin up and down, and expressing $U^{x,y}$ in terms of the Pauli matrices, $U^x \to \sigma^z, U^y \to \sigma^x$. Under this identification, Eq. (5) becomes

$$H \to 2\cos\theta \sum_i \sigma_i^z \sigma_{i+1}^z + 2\sin\theta \sum_i \sigma_i^x \sigma_{i+1}^x.$$

This is the anisotropic XZ model, which is gapped for all θ, except $\theta = \pm\pi/4$ and $\pm 5\pi/4$ where it is quantum critical. The phase diagram, which is symmetric under $\theta \to \pi/2 - \theta$ due to duality, is shown in Fig. 2(a). In the gapped phases, the $\mathcal{U}^x/\mathcal{U}^y$ and/or the translation symmetry is spontaneously broken, leading to twofold ground-state degeneracy. At the points $\theta = \pm\pi/4$ and $\theta = \pm 5\pi/4$, the ground state respects all symmetries but the energy spectrum is gapless.

To get a qualitative understanding of how this phase diagram generalizes to other values of m, it is instructive to consider four special points. First, for $\theta = \pi$, the Hamiltonian becomes classical because there are no noncommuting operators. In that case, the ground state is given by $\prod_{i=1}^L |q\rangle$ and is m-fold degenerate for any given m. Clearly the $\mathcal{U}^y$ symmetry is spontaneously broken and there is an energy gap. The gap persists for small $\theta - \pi$, which shows that this is an extended gapped phase. For $m = 2$, it extends to the full interval $3\pi/4 < \theta < 5\pi/4$, with an equivalent, dual phase in the interval $5\pi/4 < \theta < 7\pi/4$.

Provided m is even, the situation is similar at the point $\theta = 0$. In that case, the ground state is also m-fold degenerate, now with a ground state of the form $\prod_{i=1}^L |(-1)^i q\rangle$. Also around the point $\theta = 0$, there is a gapped phase, with a ground state that in the $L \to \infty$ limit, spontaneously breaks both $\mathcal{U}^y$ and translational symmetry. For $m = 2$, this phase also extends to the full interval $-\pi/4 < \theta < \pi/4$, with the equivalent, dual phase in the interval $\pi/4 < \theta < 3\pi/4$.

However, if m is odd, the situation is quite different. For $\theta = 0$, all states with

$$q_i - q_{i+1} = (m \pm 1)/2 (\mathrm{mod}\ m)$$

yield the same energy. As a result, the ground state is extensively degenerate. For example, in an open chain, the degeneracy is $2^{L-1} m$. When θ deviates from zero, these degenerate configurations are mixed by the $\sin\theta$ term, and hence the degeneracy is lifted. This is very similar to the effects of quantum fluctuations in frustrated magnets. Due to the duality of the Hamiltonian, the same discussions hold for $\theta = \pi/2$, except the roles of q and $\tilde{q}$ are interchanged.

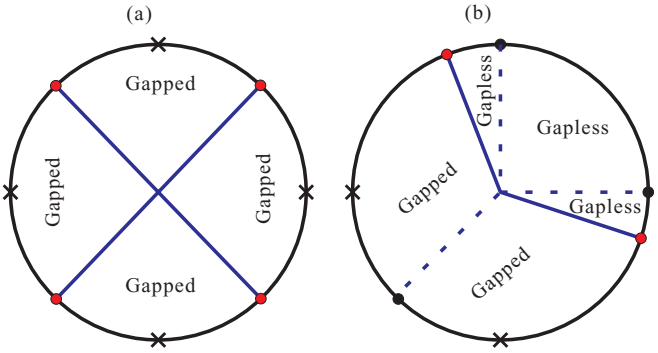

FIG. 2. (Color online) The phase diagrams of Eq. (5) for (a) $m = 2$ and (b) $m = 3$. The black and red dots mark first-order transitions and critical points, respectively. At points marked by crosses, the model is classical and hence exactly solvable.

IV. THE CASE $m = 3$

In the previous section, we used symmetry considerations to gain knowledge about the behavior of the model at some special points, and some general properties of the phase diagram. In this section, we will focus on the case $m = 3$. We start by giving a quick overview of the phase diagram in Sec. IV A, followed by a more detailed description of the various phases and phase transitions in the subsequent sections.

A. Overview of the $m = 3$ phase diagram

We first show the exact diagonalization results of a small system (namely, $L = 12$ sites). In Fig. 3, the ground-state energy per site is shown in the upper panel, while the first derivative is given in the lower panel.

The figures give a clear indication of a first-order transition, due to a level crossing, at $\theta = 0$. This is signaled by a sharp kink in the ground-state energy. As already discussed, there is at this point also an extensive ground-state degeneracy, which grows exponentially with the system size. Due to the "duality symmetry," there is an analogous first-order transition at $\theta = \pi/2$.

This first-order transition connects two gapless phases. In fact, we will later show that throughout the whole region $0 < \theta < \pi/2$, the system is critical and characterized by a central charge $c = 2$. This region contains the special point $\theta = \pi/4$, where the Hamiltonian is self-dual. Moreover, we will show in the next section that the critical behavior for $\theta \lesssim 0$ can be related to that for $\theta \gtrsim 0$ (and similarly the behavior for $\theta \gtrsim \pi/2$ is related to that of $\theta \lesssim \pi/2$). The critical region for $\theta > \pi/2$ gives way to a gapped phase at around $\theta \approx 0.6\pi$, which is signaled by a sudden drop in the first derivative of the ground-state energy; see Fig. 3. A much more detailed study of this phase transition will be given in Sec. IV D.

Beyond $\theta \approx 0.6\pi$, and in fact in the whole region $0.6\pi \lesssim \theta < 5\pi/4$, the system is gapped, with a threefold degenerate ground state in the thermodynamic limit. In this gapped phase, the $\mathcal{U}^y$ symmetry is spontaneously broken. The property of this

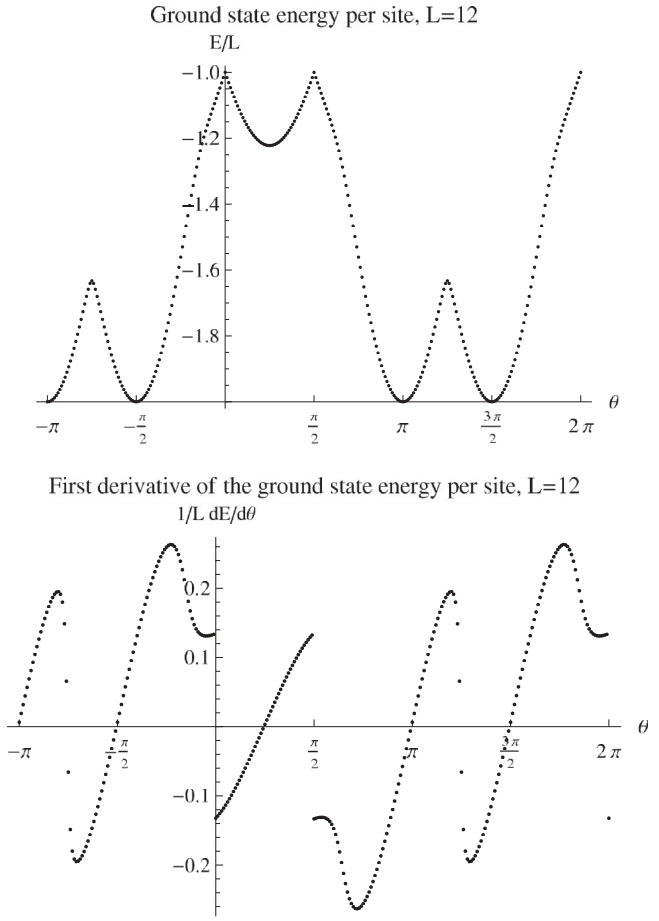

FIG. 3. Upper panel: Ground-state energy per site of the $m = 3$ model for $L = 12$ sites, as a function of the angle θ. Lower panel: First derivative of the ground-state energy per site of the $m = 3$ model for $L = 12$ sites, as a function of the angle θ.

phase can be understood by considering the special point $\theta = \pi$, where the Hamiltonian has no noncommuting operators and can trivially be solved.

The gapped phase in the region $0.6\pi \lesssim \theta < 5\pi/4$ has its dual analog in the region $5\pi/4 < \theta \lesssim 1.9\pi$, where the $\mathcal{U}^x$ symmetry is spontaneously broken, giving rise to a threefold degenerate ground state. In addition to the above, the two panels in Fig. 3 also give hints of a phase transition between the two gapped phases at $\theta = 5\pi/4$. Section IV F is devoted to a more detailed discussion of this phase transition.

B. The behavior near $\theta = 0$

Next, let us focus on $\theta \approx 0$, and for simplicity let us concentrate on $m = 3$. The arguments given below can be applied for arbitrary odd m. As discussed above, the ground states of the $\cos\theta$ term of the Hamiltonian consist of $|\{q_i\}\rangle$ configurations where no nearest neighbors have the same q. We shall refer to the subspace spanned by these configurations as the projected space. For small θ, the $\sin\theta$ term of the Hamiltonian mixes different configurations within the projected space and also mixes states in the projected space with those outside. However, since there is an energy gap separating the projected space from the rest of the Hilbert space, the effective low-energy Hamiltonian, derived in degenerate perturbation theory to lowest order in $\sin\theta$, is identical to the projection of H on the projective space. The Hamiltonian, with the ground-state energy at $\theta = 0$ subtracted, can be written as

$$H = \sin\theta \mathcal{P} \sum_i P_{i,i+1} \mathcal{P}, \tag{6}$$

where $\mathcal{P}$ projects states into the projected space, $P_{i,j}$ exchanges q_i and q_j, and the factor $\sin\theta$ defines simply an overall energy scale.

The projected Hamiltonian is symmetric under the same discrete group as the full Hamiltonian. However, it has two additional continuous U(1) symmetries. These symmetries are generated by the conserved charges N_q, which measure the number of sites with the given value of q. Due to the constraint $\sum_{q=0}^{2} N_q = L$, only two of the charges are independent.

The spectrum of Eq. (6) is invariant upon a global sign reversal of the Hamiltonian. The way to show this is to consider a division of the projected space into invariant subspaces, where each of these is spanned by tensor products of q-basis vectors, all having the same numbers $N_{0,1,2}$. The states within such a subspace can all be mapped into each other by a permutation of the set of q values. A further subdivision is achieved by collecting all states that are connected by *even* permutations in one group. This defines two smaller subspaces, with basis vectors that are interconnected by odd permutations. One can define a unitary operator Γ_z that takes the value 1 in one of the subspaces and -1 in the other. Since the Hamiltonian (6) is the sum of transposition operators, it only has nonvanishing matrix elements between states with different values for Γ_z. This means that H anticommutes with Γ_z, hence, the eigenspectrum of H is symmetric about $E = 0$. Upon $\theta \to -\theta$, the Hamiltonian in Eq. (6) reverses sign. However, the eigenspectrum remains unchanged.

Now let us come back to the full Hamiltonian. Near $\theta = 0$, the low-lying energy spectrum changes linearly with $\sin\theta$. Therefore, there is a massive crossing of energy levels, with no level repulsion, at $\theta = 0$. In particular, the ground state changes abruptly, consistent with a first-order transition at $\theta = 0$ in the thermodynamic limit ($L \to \infty$).

The above discussion is in reality not restricted to $m = 3$, but applies to all odd integer m. Thus, to lowest order in the deviation from $\theta = 0$, the low-energy Hamiltonian, for $m = 2n + 1$, can be written as a projected Hamiltonian of the same form as Eq. (6). Similarly, one can show that there are now $m - 1$ conserved quantities, specified by the numbers $N_0, \ldots, N_{m-1}$. The spectrum is inverted in the same way when $\theta \to -\theta$, and consequently, for odd integer m, there is at $\theta = 0$ a first-order phase transition. Due to the duality symmetry, there is precisely the same type of phase transition at point $\theta = \pi/2$.

C. The critical region $0 < \theta < \pi/2$

We now provide evidence for the two phases, one in the interval $0 < \theta < \pi/2$ and the other in the interval $-0.1\pi \lesssim$

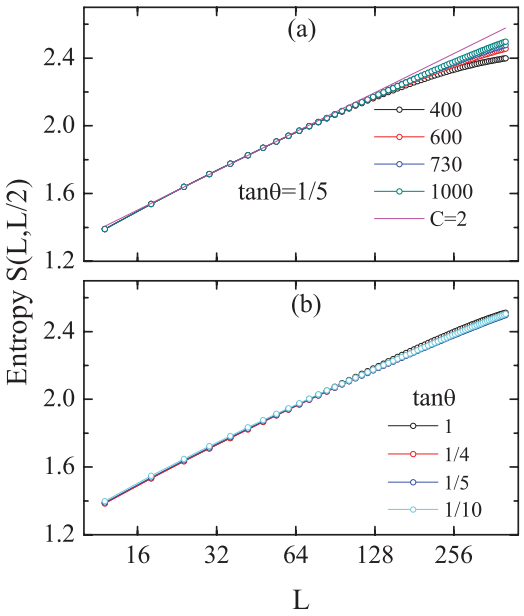

FIG. 4. (Color online) (a) The entanglement entropy associated with $\tan\theta = 1/5$ as a function of $\ln L$ under the open boundary condition. Different curves are distinguished by the different number of kept states D in the DMRG calculation. The fitting curves are constructed using $c = 2$. (b) A comparison of the entanglement entropy for $\tan\theta = 1, 1/4, 1/5, 1/10$ calculated with $D = 1000$.

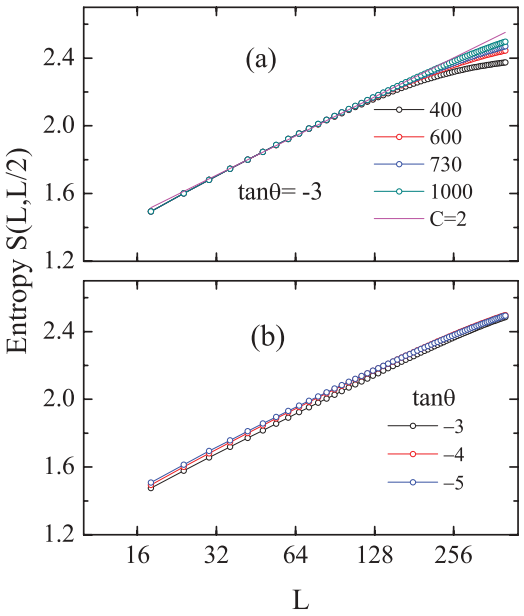

FIG. 5. (Color online) Same as Fig. 4, here with values of θ in the interval $\pi/2 < \theta \lesssim 0.6\pi$.

$\theta < 0$ ($\pi/2 < \theta \lesssim 0.6\,\pi$), which are connected by the first-order phase transition at $\theta = 0$ ($\pi/2$), to be gapless.

To determine the properties of the model in the region $0 < \theta < \pi/2$, we have calculated the entanglement entropy by DMRG.[3,4] In Fig. 4, we present a plot of the entanglement entropy S_A for a subsystem (subregion) A of length $\ell = L/2$ for various different values of θ in the interval $0 \leqslant \theta \leqslant \pi/2$. In Fig. 4(a), θ is fixed ($\tan\theta = 1/5$), while the number D of states kept during the DMRG calculation is varied. The plots show that for $L = 400$, the value obtained for $D = 1000$ has almost converged. In Fig. 4(b), we compare the results for various angles θ, keeping $D = 1000$ states in each case.

The scaling of the entanglement entropy with system size, shown in Fig. 4, is linear in $\ln L$, which indicates that for these values of θ, the model is described by a conformal field theory (CFT). For $(1+1)$-dimensional CFTs, with open boundary condition, the entanglement entropy S_A of a subsystem (subregion) A of length ℓ is $S_A = (c/6)\log[(2L/\pi a)\sin(\pi\ell/L)] + g + c_0$,[13–15] where c is the central charge associated with the critical behavior, a is a length scale, g is the boundary entropy, and c_0 is a nonuniversal constant. In our calculation, we fix ℓ to $L/2$, so that $S_A \simeq (c/6)\log(L)$ for large L.

From the numerical results, we conclude that for all values of θ studied, the system exhibits conformal invariance (and hence is gapless) with a central charge $c = 2$. This value of the central charge can be understood by noting that for small θ, there are two conserved charges, each generating an emerging U(1) symmetry. For a similar gapless phase with $c = 2$, realized in interacting boson systems on the three-leg ladder at one-third filling, see Refs. 16 and 17.

Entanglement entropy plots for the region $-0.1\pi \lesssim \theta < 0$ and $\pi/2 < \theta \lesssim 0.6\pi$ show the same picture, and, here too, we obtain $c \approx 2$, indicating gaplessness (see Fig. 5). The fact that the central charge is the same for these two θ regimes can be understood as a result of the invariance of the spectrum of Eq. (6) upon reversing the sign of the projected Hamiltonian.

To give further evidence that the system is critical, we also calculate the entanglement spectrum by means of DMRG. In particular, we consider the eigenvalues $\{\lambda_i\}$ of the density matrix. It was shown in Ref. 18 that the mean number of eigenvalues larger than a given λ, denoted by $n(\lambda)$, can be calculated from CFT, with the result

$$n(\lambda) = I_0[2\sqrt{b\ln(\lambda_{\max}/\lambda)}], \tag{7}$$

where $I_k(x)$ is the modified Bessel function of the first kind, $b = -\ln(\lambda_{\max})$, and $\lambda_{\max}$ is the largest eigenvalue of the reduced density matrix.

In Fig. 6, we plot the distribution of the λ_i for two points in the gapless region. Concretely, we plot the value of the ith eigenvalue, following Ref. 18. The data agrees with the CFT result asymptotically, which confirms that the gapless phase can be described by CFT. In principle, it should be possible to extract more information about which CFT describes our system from the distribution of the small eigenvalues of the reduced density matrix, but this is a difficult task, which we leave for future investigations.

Numerical studies of energy gaps between low-lying levels confirm the picture of gapless phases in the intervals referred to above. The DMRG evaluations of the gaps show a clear $1/L$ scaling behavior, consistent with a conformal field theory limit when $L \to \infty$. As we already have pointed out, the numerical plots of the θ dependence of the ground-state energy show a discontinuity in the derivative at the points $\theta = 0$ and $\theta = \pi/2$, consistent with a first-order phase transition at these points.

The space of $c = 2$ conformal field theories is rather extensive; see Ref. 19 for an overview of possible theories. In the past, in order to identify the low-energy conformal field theories of lattice models, it has been very instructive to study

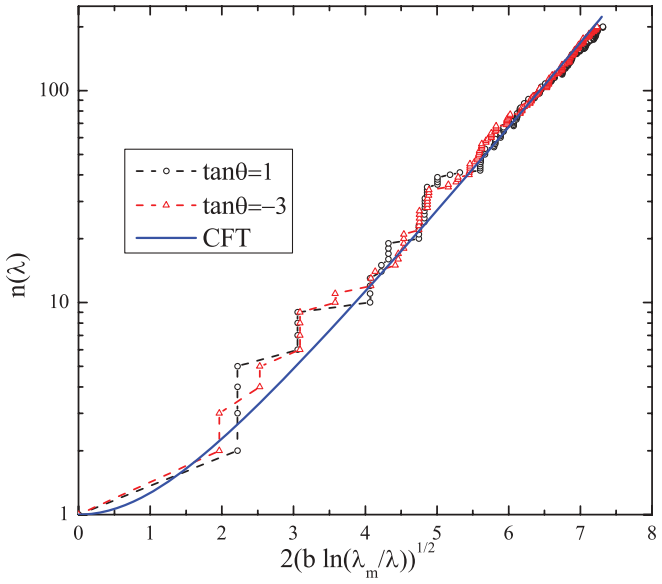

FIG. 6. (Color online) The distribution of the eigenvalues of the density matrix λ. The length of the chain is 102 and the number of states kept in the DMRG is 1000. The blue solid line is the prediction of CFT. The step structure in the calculated data is due to the degeneracies of the eigenvalue of the reduced density matrix.

the models under periodic boundary conditions and to calculate the energy spectra as functions of the various momenta. This can give crucial information in identifying the type of critical behavior. For the torus model, we give in Fig. 7 the energy spectra, resolved with respect to momentum, for $\theta = \pi/4$ and for system sizes $L = 12$ and $L = 18$.

From conformal field theory, it follows that if a system is critical, then the energies of the low-lying states are given by

$$E = E_0 L + \frac{2\pi v}{L}\left(h_{\mathrm{L}} + h_{\mathrm{R}} - \frac{c}{12}\right). \tag{8}$$

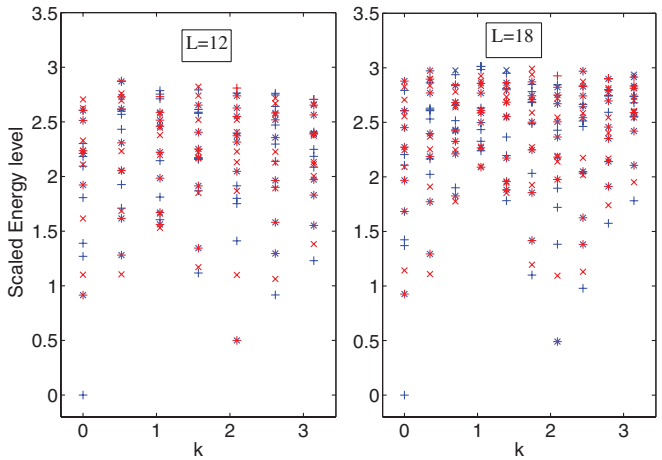

FIG. 7. (Color online) The momentum-resolved spectrum at $\theta = \pi/4$, for $L = 18$. The blue plusses correspond to the singlets $(Q, \tilde{Q}) = (0,0)$; the red crosses correspond to the quadruplets $(Q, \tilde{Q}) = (1,1); (1,2); (2,1); (2,2)$; and the blue cross, red plus combinations correspond to $(Q, \tilde{Q}) = (0,1); (0,2); (1,0); (2,0)$.

In this equation, E_0 is a constant energy per site, v is a characteristic velocity, c is the central charge, and h_{L}, h_{R} are the left and right scaling dimensions of the associated field in the CFT. In our case, we know from the DMRG results that $c = 2$. Furthermore, from studies of the L dependence of the ground-state energy, which has $h_{\mathrm{L}} = h_{\mathrm{R}} = 0$, the velocity parameter v has been determined. In Fig. 7, the energies are shifted such that the ground state has zero energy, and the energies are rescaled in units such that $2\pi v/L = 1$.

Scaling operators in CFT are grouped in terms of primary fields, with total scaling dimension $h_{\mathrm{L}} + h_{\mathrm{R}} = \Delta_p$, and their descendants, with $h_{\mathrm{L}} + h_{\mathrm{R}} = \Delta_p + n$, where n is a positive integer. When the low-energy spectrum is presented in the form shown in Fig. 7, one should, in principle, be able to identify the CFT through the position Δ_p of the primary fields, with their associated towers of descendent state. However, in our case, we have not been able to make such an identification. In part that is due to the wide range of possibilities for $c = 2$, as discussed in Ref. 19, but also due to finite size effects for the systems for which we are able to perform exact diagonalization. Thus, the low-energy spectra show several characteristics of a critical system, but we have not been able to conclusively identify which $c = 2$ conformal field theory describes the critical behavior.

D. The phase transitions at $\theta \approx 0.6\pi$ and $\theta \approx -0.1\pi$

The numerics indicate that a phase transition to a gapped phase, with a threefold degenerate ground state, takes place at $\theta \approx -0.1\pi$, with a similar transition at $\theta \approx 0.6\pi$. These two gapped phases, which are connected by the duality transformation, seem to cover the parameter range $0.6\pi \lesssim \theta \lesssim 1.9\pi$. We will come back to these gapped phases in the next section.

Figure 8(a) shows the numerical estimate of the location of the critical point between the gapless phase and gapped phase in the vicinity of $\theta \approx 0.6\pi$. In the plot, the critical point is marked by the crossing between two excitation energies for different values of L. The curve labeled "gap in $Q = 0$ sector" is the energy difference between the ground state and the lowest excited state in the $Q = 0$ sector, while the curve labeled "$E_g(Q = 1) - E_g(Q = 0)$" gives the gap between the lowest-energy state in the $Q = 1$ sector and the ground state. In the gapped phase, the excited $Q = 0$ state will merge with the ground state in the limit $L \to \infty$, but in the gapless phase, it lies above the lowest-energy state in the $Q = 1$ sector. Thus a crossing between the two excited states takes place at a point which moves towards the phase-transition point as $L \to \infty$. The plot shows a convergence of the crossing towards a point slightly below $\theta = 0.61\pi$. A plot of the second derivative of the ground-state energy through this point, as shown in Fig. 8(b), indicates that a continuous phase transition is taking place. It is worthy to note that the continuous phase transitions in question link a gapless phase and a gapped phase. This is different from usual quantum phase transitions where the phases on both sides are gapped. It is similar to the Kosterlitz-Thouless phase transition, except the central charge is different.

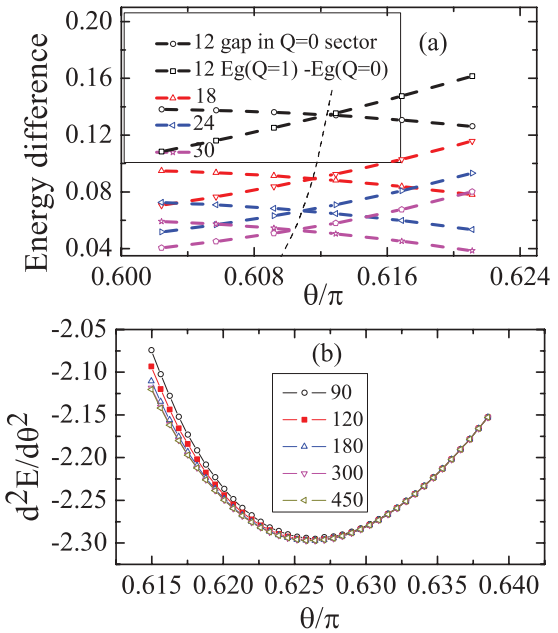

FIG. 8. (Color online) (a) The crossing between the ground state in $Q = 1$ and the first excited state in the $Q = 0$ sector. Different color indicates different lattice size. (b) The second derivative of ground-state energy with respect to θ.

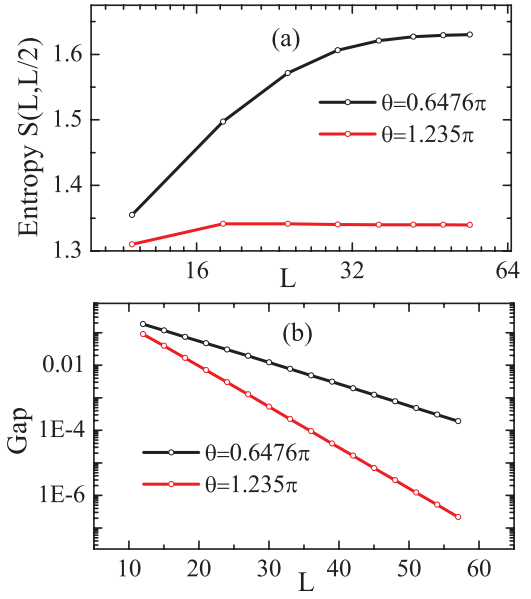

FIG. 9. (Color online) (a) The entanglement entropy for two different θ in the gapped region. The entropy saturates as $\ln L$. (b) The energy difference of the first excited state and the ground state in the $Q = 0$ sector. The finite-size gap decays exponentially to 0 with increasing L.

E. The gapped phases

We now focus our attention on the gapped phases of the $m = 3$ quantum torus model. A first gapped phase extends from the phase transition near $\theta \approx 0.6\pi$ to $\theta = 5\pi/4$. The second gapped phase is dual to the first one, and ranges from $\theta = 5\pi/4$ to $\theta \approx 1.9\pi$. We will discuss the phase transition between these two gapped phases in the following section.

To understand the symmetry breaking in the gapped phase, it is useful to consider the special points $\theta = \pi$ and $\theta = 3\pi/2$. For these values of θ, the Hamiltonian becomes classical (i.e., there are no noncommuting operators), where the ground state is exactly threefold degenerate even for finite L. Away from these points, there is finite-size lifting of the ground-state degeneracy. However, the latter decreases exponentially with increasing L. In Fig. 9(a), the presence of a gap is demonstrated via the saturation of the entanglement entropy as a function of $\ln L$. The exponential decay of the finite-size gap between the states, which evolve into the ground state, is shown in Fig. 9(b).

At the special points $\theta = \pi$, the threefold degenerate ground state is spanned by the product states $\prod_{i=1}^{L} |q\rangle$, $m =$ 1,2,3. As a consequence, the correlation function $\langle U_i^{x\dagger} U_j^x \rangle$ is simply a constant, while the corresponding U^y correlation function vanishes for $i \neq j$. Even if this is a very special situation, a similar behavior of the correlations functions is seen in the full gapped phase, up to $\theta = 5\pi/4$. Thus, the U^x correlation function is long range, while the U^y correlation function decays exponentially with the distance between the two points i and j. This is shown for a particular value $\theta = 1.265\pi$ in Fig. 10 for a system of length $L = 102$. At the point $\theta = 5\pi/4$, there is an interchange between the correlations of U^x and U^y, as follows from the duality symmetry. The curve corresponding to $\theta = 5\pi/4$ in Fig. 10 shows identical long-range correlations for U^x and U^y. This can be understood as due to the fact that the ground state for any finite L is a 50/50 superposition of two states, with correlations that are symmetric under the interchange $x \leftrightarrow y$.

F. The phase transition at $\theta = 5\pi/4$

As a final point, we have examined the phase transition at the point $\theta = 5\pi/4$, at which the two gapped phases meet. In the vicinity of $\theta = 5\pi/4$, there are six energy eigenstates

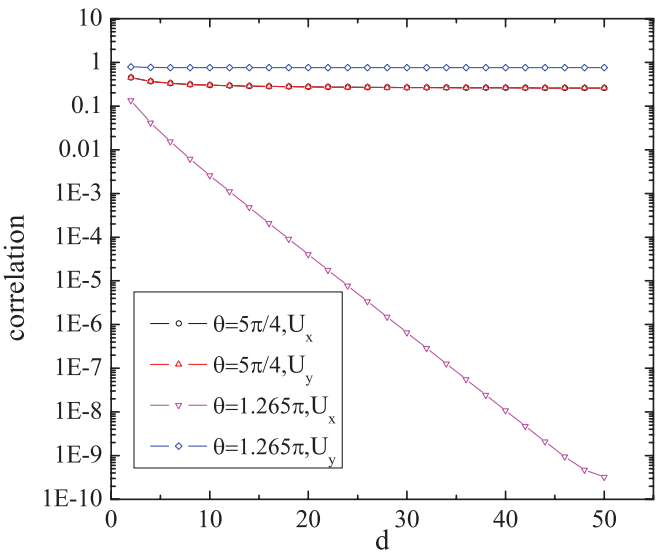

FIG. 10. (Color online) Logarithmic plot of the U^x and U^y correlations at $\theta = 5\pi/4$ and $\theta = 1.265\pi$. For $\theta = 5\pi/4$, the two curves fall on the top of each other. d is the distance between the two points for which the correlation is calculated. The system size used in the calculation is $L = 102$.

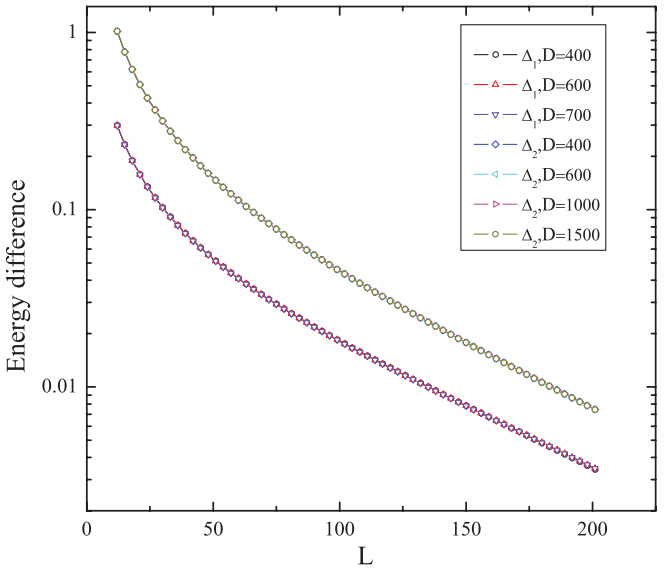

FIG. 11. (Color online) The exponential decay of the energy difference between the two lowest levels and the ground state at $\theta = 5\pi/4$. Δ_1 is the energy difference between the first excitation level (a quadruplet; see the main text) and the ground state (a singlet), and Δ_2 is the energy difference between the second excitation level (also a singlet) and the ground state. They both decay to zero exponentially with system size L.

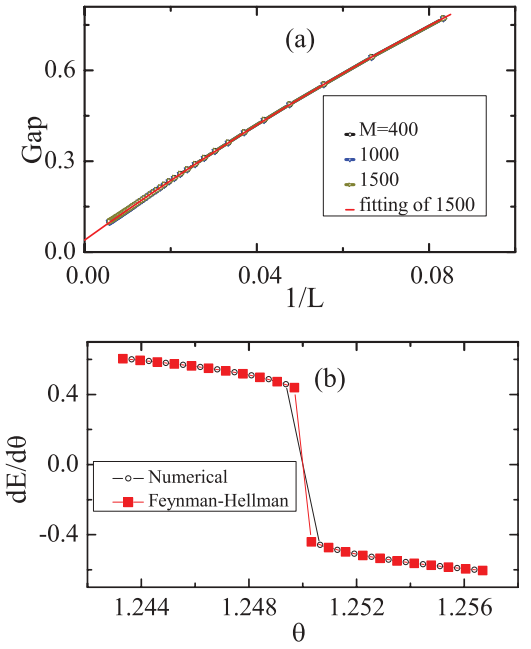

FIG. 12. (Color online) (a) The energy difference between the first excited state and the ground state in the $Q = 1$ sector at $\theta = 5\pi/4$. We use a quadratic fitting of the gap with $1/L$ using the $D = 1500$ data. As L goes to infinity, there is a small gap ($\sim$0.04). (b) The first derivative of the ground-state energy with respect to θ. The circle results are derived by the numerical differential of the ground-state energy, while the square data are derived directly by using the Feynman-Hellman theorem.

that are important: two $(Q,\tilde{Q}) = (0,0)$ singlets, a $(Q,\tilde{Q}) = (0,1);(0,2)$ doublet, and another $(Q,\tilde{Q}) = (1,0);(2,0)$ doublet. All of the numerical evidences are consistent with the following picture in the thermodynamic limit. For $\theta < 5\pi/4$, the ground state is triply degenerate. The triplet involves one of the $(Q,\tilde{Q}) = (0,0)$ singlets and the $(Q,\tilde{Q}) = (0,1);(0,2)$ doublet. For $\theta > 5\pi/4$, the ground state is also triply degenerate. This time the triplet involves the other $(Q,\tilde{Q}) = (0,0)$ singlet and the $(Q,\tilde{Q}) = (1,0);(2,0)$ doublet. At $\theta = 5\pi/4$, the two triplets cross, resulting in a sixfold degenerate ground state. For finite L, the doublet $(Q,\tilde{Q}) = (0,1);(0,2)$ precisely degenerates with $(Q,\tilde{Q}) = (1,0);(2,0)$. This is because they form the four-dimensional irreducible representation of the enlarged symmetry group at the self-dual point. In contrast, the two $(Q,\tilde{Q}) = (0,0)$ singlets are slightly split due to avoided crossing caused by the finite system size. The above picture suggests a first-order phase transition at the self-dual point in the thermodynamic limit. This is caused by the crossing of energy levels. The two phases are distinguished by different long-range correlations for either U^x or U^y, as previously discussed.

The character of the phase transition is further illustrated by the plots in Figs. 11, 12, and 13. In Fig. 11, we display the behavior of the gap at the transition point $\theta = 5\pi/4$. The ground state is a $(Q,\tilde{Q}) = (0,0)$ singlet, and Δ_1 denotes the energy difference with the first excited "level," which is the $(Q,\tilde{Q}) = (0,1);(0,2);(1,0);(1,0)$ quadruplet (see the discussion above). Δ_2 denotes the energy difference between the ground state and the second excited level, which is again a $(Q,\tilde{Q}) = (0,0)$ singlet. The energy differences Δ_1 and Δ_2 are given in Fig. 11 for various values of D, with the number of states kept in the DMRG, clearly showing that the results have converged as a function of D. Both the energies of the first and second excited levels decay exponentially with system size, which implies a sixfold degenerate ground state, because other levels have a finite gap to these six degenerate states in the thermodynamic limit; see also Fig. 12.

Figure 12(a) shows the behavior of the energy difference between the two lowest-lying levels in the $Q = 1$ sector. The

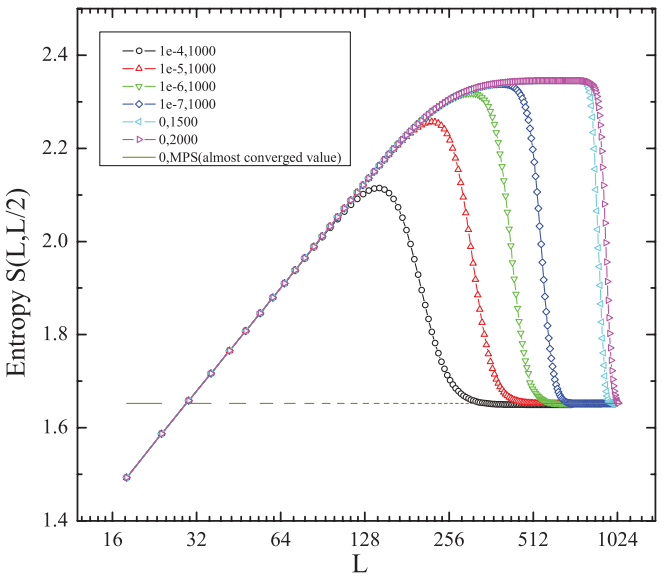

FIG. 13. (Color online) The entanglement entropy, close to the point $\theta = 5\pi/4$, as obtained from DMRG and the MPS method.

latter does not merge with the degenerate ground state in the thermodynamic limit. The plot shows that a small energy gap remains as $L \to \infty$.

In Fig. 12(b), the first derivative of the ground-state energy is plotted as a function of θ. It shows a sharp drop at $\theta = 5\pi/4$, which is expected to become infinitely sharp in the limit $L \to \infty$ because the transition happens at an isolated point between two gapped phases. The sharp change in the derivative of the ground-state energy is consistent with the picture of the phase transition as caused by the crossing of the two lowest-energy levels.

In Fig. 13, we show the results of a detailed study of the behavior of the entanglement entropy, near the point $\theta = 5\pi/4$. The plot shows that for system size up to about $L = 256$, the entanglement entropy behaves as expected for a critical point, and is consistent with $c = 2$. For larger system sizes, the entanglement entropy flattens off, and finally crosses over to the (lower) value obtained via the MPS method. This last crossing over happens at larger system size, if the number of states kept in the DMRG calculation is increased, although for $D = 2000$, the numerics seems to have converged.

The drop in the entanglement entropy for large L, at $\theta \sim 5\pi/4$, can be understood in terms of the level-crossing picture as follows: There are two states with $(Q, \tilde{Q}) = (0,0)$ participating in the crossing; let us denote them $|\psi_-\rangle$ and $|\psi_+\rangle$, where $|\psi_-\rangle$ ($|\psi_+\rangle$) is a ground state for $\theta < 5\pi/4$ ($\theta > 5\pi/4$). They are not orthogonal, but the overlap is exponentially suppressed for large L. For finite L, the true ground state is a mixture of $|\psi_-\rangle$ and $|\psi_+\rangle$, which at $\theta = 5\pi/4$ is an equal superposition thereof. Away from this point, the ground state rapidly rotates into either $|\psi_-\rangle$ or $|\psi_+\rangle$, depending on whether θ is reduced or increased from $\theta = 5\pi/4$. This rotation is more rapid the larger L is, so that for $L \to \infty$, the crossing between $|\psi_-\rangle$ and $|\psi_+\rangle$ becomes sharp. Assume we choose θ slightly smaller than $5\pi/4$. For small L, the ground state is essentially the 50% mixed state, but when L increases at some point, it rapidly changes to $|\psi_-\rangle$. The entanglement entropy of each of the two states, $|\psi_+\rangle$ and $|\psi_-\rangle$, clearly is smaller than that of the superposition of the two. Due to the symmetry between $|\psi_-\rangle$ and $|\psi_+\rangle$ at $\theta = 5\pi/4$, and the rapid decay of the overlap between them as $L \to \infty$, we can in fact estimate the drop in entanglement entropy. Since each of the two states in the superposition gives equal contributions to the entanglement entropy, the drop should be close to $\ln 2$. The numerical value found for the curves plotted in Fig. 13 is in fact very close to $\ln 2$.

We have conclusively shown that the gap at the transition point at $\theta = 5\pi/4$ does not close, and that that system exhibits long-range order. It is intriguing to observe that the scaling of the entanglement entropy shows behavior consistent with $c = 2$ critical behavior up to fairly large system sizes of at least $L = 200$ (due to the rather large correlation length). Combined with exact diagonalization results (which we performed up to $L = 18$; not shown), one could incorrectly be led to believe that the system is critical. It would be interesting to investigate if the system can be (fine) tuned to become critical by perturbing away from the gapped $\theta = 5\pi/4$ point. One could, for instance, allow complex amplitudes in the Hamiltonian (5) or mixed terms such as $U_i^x U_{i+1}^y$.

V. CONCLUSIONS

To summarize, we have presented a class of one-dimensional lattice models, called the quantum torus chain. These models depend on an integer-valued parameter m (the number of magnetic flux quanta piercing through each torus), which controls the presence or absence of frustration. In addition, there is a continuous parameter θ which controls the ratio of the noncommuting terms in the Hamiltonian. The models show a variety of gapless and gapped phases. In all cases, the gapped phases break symmetries of the Hamiltonian. We characterize these gapped phases based on the properties of specific points in parameter space, where the Hamiltonian is exactly solvable. For the gapless phases, we have used DMRG and matrix product state methods to evaluate the entanglement entropy and hence deduce the central charge.

Based on these analyses, we have concluded that for even m, the system is generically gapped with isolated quantum critical points separating different gapped phases. For odd m, there exist extended regions in the parameter θ where the system is gapless. The above general conclusion is motivated by the mapping of the $m = 2$ model on the spin-1/2 XZ model, and the detailed numerical studies of the $m = 3$ model. For the latter, the quantum phase transitions between two gapless or two gapped phases are first order, while the transitions between the gapless and gapped phases are continuous. Consistent with these conclusions, we have numerical evidence from studies of the $m = 4$ model that this is also gapped in the first quadrant $0 < \theta < \pi/2$.

Our study raises a series of open questions. At the moment, we have not been able to pin down the conformal field theory for the $c = 2$ gapless phases of the $m = 3$ model. Of course, gapless phases have precedents in one dimension (e.g., the Luttinger liquid).[20] However, gapless *phases* in more than one dimension are very unusual. Our model, of course, can be defined in any spatial dimension.

Without going into much detail, we can say that for m even, there is no frustration, and at the special angles $\theta = 0, \pi/2, \pi, 3\pi/2$, the ground states are direct product states, with a finite degeneracy. Thus, at least near these points, we expect the system to be gapped. Whether or not these gapped phases extend over the full parameter space, leaving only critical points, as is the case in our 1D model, needs further investigation. For odd m, there is also quantum frustration in higher dimensions. It is interesting to ask whether the gapless phase still exists in higher dimensions.

There are several ways to extend our model. One could try to include terms which mimic a magnetic field in ordinary spin chains. In our model, the closest analog of a magnetic field would be a one-site term, which breaks the symmetry of the model, by favoring (say) one of the possible states. More phase transitions should be expected in this enlarged parameter space because a strong symmetry-breaking term will simply "polarize the degrees of freedom," leading to ordered phases.

The general properties that we find in this work are consistent with the results discussed by Chen *et al.*[1] for systems where the internal symmetry group is represented locally on each site by a projective representation. It will be interesting to consider generalizations of the torus model where the symmetry is represented linearly locally. In this case, symmetry-protected topological states become possible.

Finally, it is interesting to ask whether it is possible to describe the gapless phase in terms of a discrete nonlinear σ model with a topological term. We will leave these and other related questions as interesting projects for future investigation.

ACKNOWLEDGMENT

D.H.L. is supported by the US DOE Grant No. DE-AC02-05CH11231.

[1]X. Chen, Z.-C. Gu, and X.-G. Wen, Phys. Rev. B **83**, 035107 (2011).
[2]F. D. M. Haldane, Phys. Lett. A **93**, 46 (1983); Phys. Rev. Lett. **50**, 1153 (1983).
[3]S. R. White, Phys. Rev. Lett. **69**, 2863 (1992).
[4]U. Schollwock, Rev. Mod. Phys. **77**, 259 (2005).
[5]G. Vidal, Phys. Rev. Lett. **98**, 070201 (2007); R. Orus and G. Vidal, Phys. Rev. B **78**, 155117 (2008).
[6]T. T. Wu and C. N. Yang, Nucl. Phys. B **107**, 365 (1976).
[7]M. F. Atiyah and I. M. Singer, Ann. Math. **87**, 484 (1968).
[8]J. Zak, Phys. Rev. **134**, A1602 (1964).
[9]C. K. Lai, J. Math. Phys. **15**, 1675 (1974); B. Sutherland, Phys. Rev. B **12**, 3795 (1975); V. I. Vichirko and N. Y. Reshetikhin, Theor. Math. Phys. **56**, 805 (1983).
[10]I. Affleck, M. Oshikawa, and H. Saleur, J. Phys. A **34**, 1073 (2001).
[11]G. Ortiz, E. Cobanera, and Z. Nussinov, Nucl. Phys. B **854**, 780 (2012).
[12]T. Mansson, J. High Energy Phys. 06 (2007) 010.
[13]C. Holzhey, L. Larsen, and F. Wilczek, Nucl. Phys. B **424**, 44 (1994).
[14]V. E. Korepin, Phys. Rev. Lett. **92**, 096402 (2004).
[15]P. Calabrese and J. Cardy, J. Stat. Mech. (2004) P06002.
[16]M. S. Block, R. V. Mishmash, R. K. Kaul, D. N. Sheng, O. I. Motrunich, and M. P. A. Fisher, Phys. Rev. Lett. **106**, 046402 (2011).
[17]R. V. Mishmash, M. S. Block, R. K. Kaul, D. N. Sheng, O. I. Motrunich, and M. P. A. Fisher, Phys. Rev. B **84**, 245127 (2011).
[18]P. Calabrese and A. Lefevre, Phys. Rev. A **78**, 032329 (2008).
[19]S. Dulat and K. Wendland, J. High Energy Phys. 06 (2000) 012.
[20]F. D. M. Haldane, J. Phys. C **14**, 2585 (1981).